

Effect of Geofoam Inclusion on Deformation Behavior of Buried Pipelines in Cohesive Soils

A.S. Mane¹(✉), Shubham Shete², and Ankush Bhuse²

¹ Department of Civil Engineering, CSMSS,
Aurangabad 431005, Maharashtra, India
abhinavmane@gmail.com

² DIEMS, Aurangabad 431005, Maharashtra, India
shubhamshetel231@gmail.com, ankushbhuse94@gmail.com

Abstract. The response of buried pipelines in cohesive soils with and without geofoam inclusion was studied extensively in this paper. Evaluation was made with the help of small-scale model tests. A series of small-scale models was performed in a fabricated box test setup, which defines the buried pipeline in cohesive soil. Black cotton soil emerged from basaltic formation in Maharashtra region of India was chosen to represent cohesive fill over and around buried pipes maintaining the constant embedment depth. Fabricated test setup was equipped with the front transparent glass panel to facilitate the capture of particle movements in the small-scale model during the increments of the loading. A 2-inch diameter HDPE pipe was used so as to represent prototype buried pipes. Geofoam was used as a compressible inclusion varying its density and cross sectional width. Plane strain conditions were adopted for all the tests. An image analysis technique was used to evaluate the performance of the geofoam in enhancement of deformation behavior of the buried pipe. Strip loading was applied with a constant load rate of 0.1 N/Sec using a Universal Testing Machine (UTM). This facilitates the correct evaluation of dissipation of the energy due to geofoam through soil arching and compression of the geofoam. Inclusion of geofoam around buried pipe prevents the adverse effects of unforeseen excessive forces on the pipeline resulting in minimal serviceability of the pipelines, reduced cost of maintenance, and reduced losses in the system and finally the effective economical operations in adverse geotechnical conditions. A maximum reduction of 32.14% was observed in the vertical deformations of buried pipe when a 150 mm wide low density geofoam was included beneath the shallow foundation at embedment depth equal to width of the footing.

Keywords: Buried pipelines · Geofoam · Black cotton soil · Small scale modeling · Image analysis

1 Introduction

The pipelines usually buried below the ground for economic, aesthetic and environmental reasons. Generally oil and gas pipelines are designed and constructed as continuous pipelines, while water supply pipelines are constructed as segmented pipelines.

These pipelines are subjected to different types of loads like soil load, traffic load and construction loading also. Due to the temperature and pressure pipelines also change its behavior as well as different types of soil would also affect on pipeline. Several authors have put forward their studies Corey et al. (2014); Stephen (2011); (Watkins (2004); Johnson et al. (2010); Anirban De and Zimmie (2016); Lin and Chou (2012)). Behavior of fine grained cohesive soils varies greatly when it comes contact with the water. It is absolutely essential to shield from destruction the buried pipelines against differential action of loading. The different types of load may cause to unreasonable differential deformation in pipes, which may further result in damage or crack of such pipes, disruption in the transportation or intended fluids. Some of the authors have suggested the use of geofoam to protect these pipes from surrounding soil (Bilgin and Stewart (2012)). However, their research is mainly limited to the concept-based application than the actual modeling of the buried pipelines. Buried pipelines could be protected by using geofoam inclusion with varying effectiveness of several factors such as density and width of the geofoam, etc. Present study demonstrates the small-scale experimental evaluation of the buried pipelines with and without geofoam. Three different densities of geofoam was adopted in the present study along with the three different widths. The model pipe diameter and loading type were kept constant throughout the study. A strip load $0.203H$ wide (where, H is the height of the pipe embedment) was applied on each of the model test at the top surface of the soil. The width of the strip load was chosen such that the Terzaghi's failure does not extend upto the pipe embedment depth.

2 Motivation Behind Present Study

Black cotton soil is highly unreliable in nature due to presence of clay minerals especially montmorillonite. When strip load is gradually applied on soft clay, it forms a zone of punching shear failure. The punching shear failure directly transfers the load on buried pipe causes deformation in the pipe. Figure 1 shows the schematic cross section of the buried pipes with and without geofoam inclusion. The zone of punching shear extends the deformation of clay and load deposited towards the pipe. When geofoam placed below the strip footing at a certain depth, geofoam compresses and the settlement due to strip loading get distributed in the surrounding clay. This forms an uniform arching in clay which distributes the deformations in the fine grained soil above the pipe. Which further provides higher load bearing area and thus comparatively less load transferred on the buried pipe. Spreading in load transfer should heighten with compressibility of the geofoam as well as with the available volume for compression under the foundation. Higher compressibility could be achieved with decrease in geofoam density, providing higher volume change in the embedment area. Increase in width of geofoam may demonstrate possible efficacious results in load scattering. With higher width of geofoam below footing wider the spread of load and greater possibilities for clay arching, increase bearing area and shear strength development of clay. So, the present study demonstrates the evaluation of effectiveness of geofoam inclusion to reduce earth pressure on buried pipes in cohesive soil. Small-scaled experimental evaluation was performed with parametric variation in geofoam width (50, 100 and 150 mm) and geofoam density (8, 16 and 24 kg/m³).

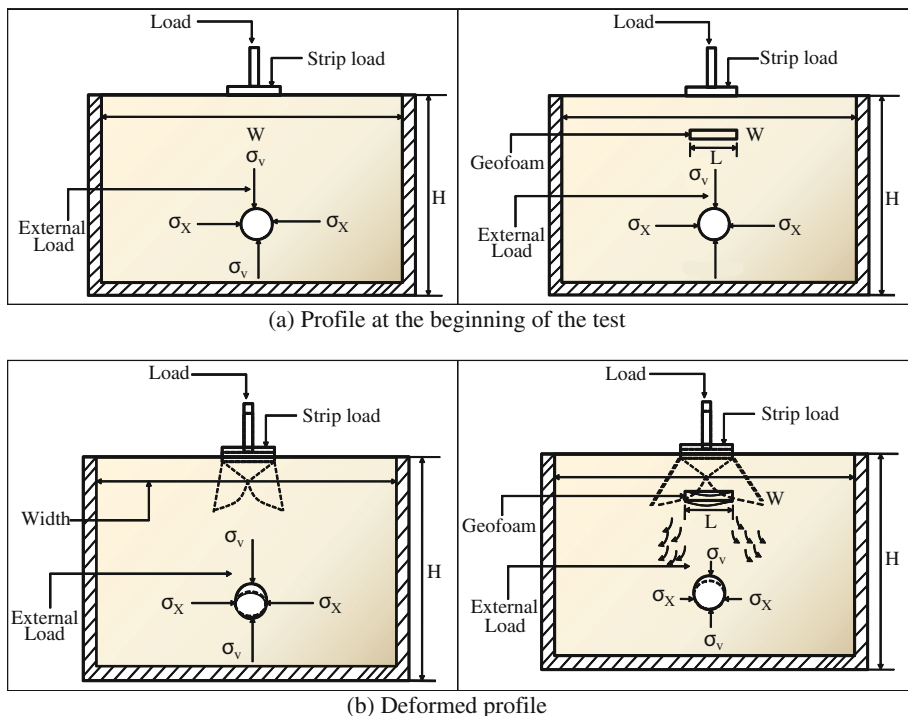


Fig. 1. Schematic cross section of buried pipe with and without geofoam

3 Model Materials

3.1 Soil

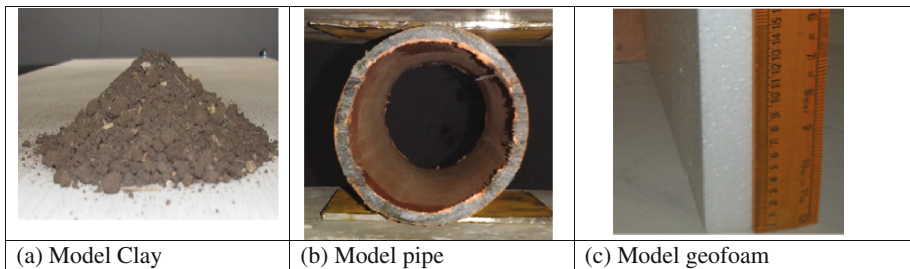
Black cotton soils are found in many part of India. The black cotton used in this study was collected from Mukundwadi, Aurangabad (Maharashtra). Black cotton soils have been identified on igneous, sedimentary and metamorphic rocks. It is mainly formed by the chemical weathering of igneous rock namely basalt. The soil is classified as high plasticity clay (CH) with expansive behavior. The optimum moisture content of black cotton was found 18% at maximum dry density of 1.56 g/cm^3 . In the present study, soil was placed at 10% wet of optimum conditions. This was obtained as dry density 1.404 g/cm^3 and moisture content 29%. Summary of properties of the model black cotton is shown in Table 1. Figure 2 (a) shows the pictorial view of collected sample of black cotton soil.

3.2 Geofoam

To represent a compressible inclusion below the shallow strip footing, expanded polystyrene (EPS) geofoam was used. EPS8, EPS16 and EPS24 types of geofoam were used in the present study with varying density 8, 16 and 24 kg/m^3 respectively.

Table 1. Properties of model materials used in present study

Particulars	Quantity		
Black cotton soil			
Soil classification	CH		
Liquid limit (%)	68		
Plastic limit (%)	26.40		
Plasticity index (%)	43.50		
Optimum moisture content (%)	18		
Maximum dry density (gr/cc)	1.56		
<u>Grain size distribution:</u>	5.1		
Sand (%)			
Silt (%)	45		
Clay (%)	49.9		
HDPE pipe			
Diameter, D _p (m)	0.05		
Compressive load at 10% strain, (kN)	26		
Geofoam			
Geofoam type	Expanded polystyrene	Expanded polystyrene	Expanded polystyrene
Geofoam legend	EPS8	EPS16	EPS24
Density (kg/m ³)	8	16	24
Compressive resistance at 2% strain (kPa)	17	42	74
Compressive elastic modulus (kN/m ²)	850	2100	3700

**Fig. 2.** Photograph view of model materials used in the present study

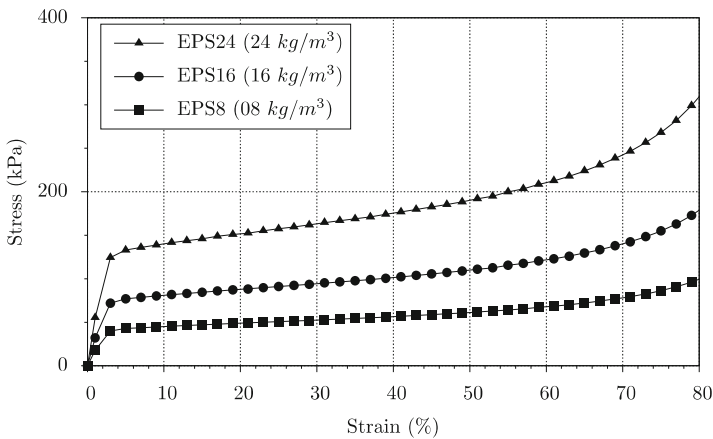


Fig. 3. Unconfined uniaxial stress strain behavior of model geofoam

The unconfined compressive resistance and elastic modulus was obtained as to be 17, 42, 74 kPa and 850, 2100 and 3700 kPa for geofoam EPS8, EPS16 and EPS24 respectively. The unconfined compressive stress strain variation for model geofoam used in the present study shown Fig. 3. Table 1 summarizes properties of the model geofoam.

3.3 HDPE pipe

The model pipe stands for the flexible buried pipeline used for water, gas and oil transportation. In the present study a commercially purchasable 2-inch diameter flexible HDPE pipe was used. Properties of the model pipe were assessed through uniaxial compression test. A simple arc arrangement was made with mild steel so as to ensure the load transfer in single vertical axis and no slippage occurs during the compression

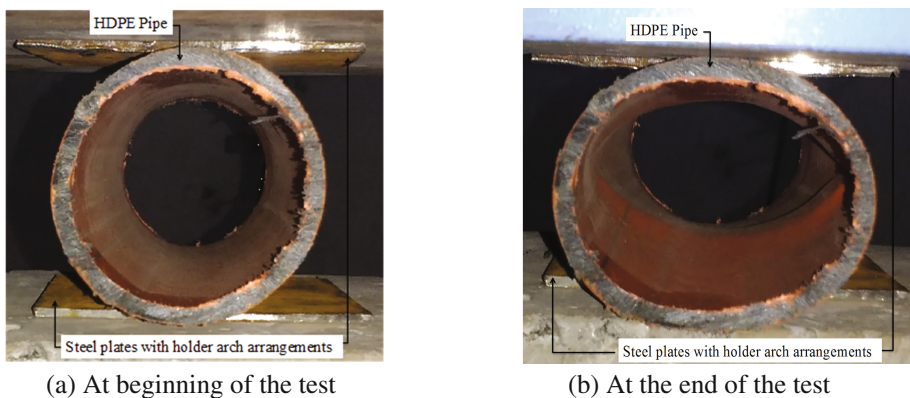


Fig. 4. Photograph view of uniaxial compression test on model HDPE pipe

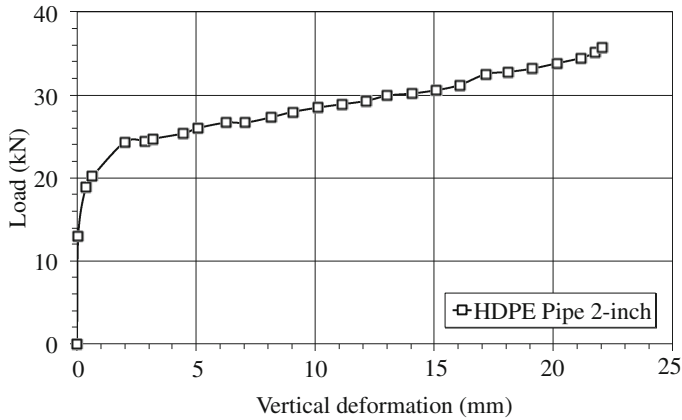


Fig. 5. Uniaxial load deformation variation of model HDPE pipe

tests. Photographic view of uniaxial compression test on model HDPE pipe used in the present study is shown in Fig. 4. Variation of load with vertical deformation of the pipe is shown in Fig. 5. Correlation of deformation to the vertical load was further used in the analysis and rendering to assess the load transferred on the pipe with and without geofoam inclusion. The loads were estimated on buried pipes based on the uniaxial load deformation information and are representative in nature. The approach followed was to evaluate the efficacy of the geofoam and limited to uniaxial tests in the present study. However, to arrive upto the accurate load transferred over the buried pipes the confined load deformation relation should be adopted, which is the future scope for the present study.

4 Model Test Package and Test Procedure

4.1 Model Test Package

The front view of the buried pipeline model constructed without and with geofoam inclusion is shown in Fig. 6. A custom designed and developed strong steel box fabrication was used for small-scale tests on buried pipelines model (with 3 MS steel walls and a glass front, shown in Fig. 6). The fabricated strong box consists of a 10 mm thick steel panel from four sides i.e. bottom, back, and side panels. A 12 mm thick glass panel was placed as the front panel to make easier the two dimensional view of the model. Movements occurring in the fine grained soil mass were captured with the help of a digital camera at a fixed time interval through this transparent front glass panel. The strong box was proof tested for its ability before starting of the tests for different soil backfills and different loading strengths. The loading intensity reaches up to the 50 kN no deformations were observed to occur in the steel panels of the strong box. Measurements were done with the help of image acquisition and analysis and deformations were checked between the box before beginning of the test and during the

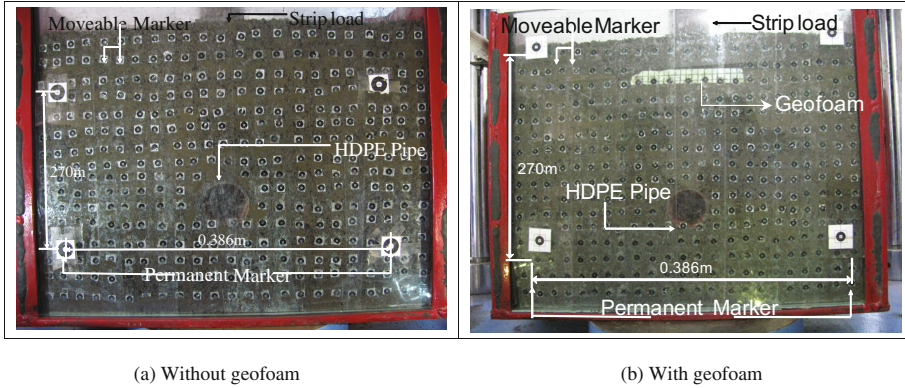


Fig. 6. Front view of the model test package

tests. The front glass panel was observed to break catastrophically, as the vertical load reaches 50 kN (characteristic value obtained based on 95% successful dummy tests). Inside the strong box numbers of thin polythene sheet strips were placed after application of grease layer. During the test polythene strips were placed such that those moves along with the soil and no boundary friction occur. A fine grained soil was placed at uniform maximum dry density 1.404 gm/cm^3 consistently for the entire test performed. A benchmark was four permanent markers, which were glued to the glass panel so as to measure movements of the moveable markers throughout the advancement of the tests. 'L' shaped plastic markers were in the soil at specific intervals to supervise the movements during the tests. PVC stand arrangement was used to hold Digital camera to make easier the undistorted supervising of the experimental buried pipeline models. EPS8, EPS16 and EPS24 three different geofoam types with varying width were used in the present study, which were placed exactly at depth equal to width of the footing (B_f) for all the model tests. Throughout the progress of the test two sets of lithium battery operated LED lighting panels were used to maintain a constant intensity of illumination.

4.2 Test Procedure

A footing was placed at the center of the test model having $0.203 H$ wide. Every test of buried pipelines models were tested under a UTM (Universal Testing Machine) at DIEMS Aurangabad with a maximum compressive and tensile capacity of 1000 kN. Load was applied in vertical direction gradually at a constant strain rate of 1.0 N/sec till the maximum settlement of 30 mm reaches or the maximum load of 30 kN reaches (whichever occurs first). Continues sequential images were taken using a Digital camera (Canon make, 9 megapixel, and enhanced shutter speed) with constant time interval equal to two second per image and at the fixed distance from the model such that the picture frame of the camera captures the full view of the model. A connected

computer stored the all images throughout the progress of the test and a few meters away from the test setup computer located.

5 Test Program

The details of the model tests performed in the present study shows in Table 2. In the study total 10 model tests were performed with and without geofoam inclusion below strip footing. Model BP11 was tested without any geofoam inclusion and it was treated as the base models for evaluation of the efficiency of the geofoam in reduction of pressure on buried pipelines in cohesive soils.

Table 2. Details of the model tests performed in the present study

Test legend	Geofoam width (mm)	Geofoam density (kg/m ³)
BP11	*N.A	*N.A
BP12	50	8
BP13	100	
BP14	150	
BP15	50	16
BP16	100	
BP17	150	
BP18	50	24
BP19	100	
BP20	150	

*Not applicable as test was performed without geofoam inclusion.

6 Analysis and Interpretation

With the help of open source software package ImageJ, deformations and strains were calculated based on particle movements in sequential images. ImageJ provides analysis and interpretation modules on a set of images. A wide range of measurements are possible on sequential images with software ImageJ. Different macros can be written to formulate a repetitive analysis on the particle movements in the images. With the help of comparative successive analysis in consecutive images, a reference measurement could be made at various points in the images. Using a Template matching, ROI (Region of interest), PIV (Particle image velocimetry) analysis all particle movements could be tracked with incremental images with progress in the test. By using the advanced Template matching and PIV (Particle Image Velocimetry) the displacements occurred in buried pipe was depicted. The deformed profile of buried pipe with surrounding cohesive soil with and without geofoam for strip loading represented in Fig. 7.

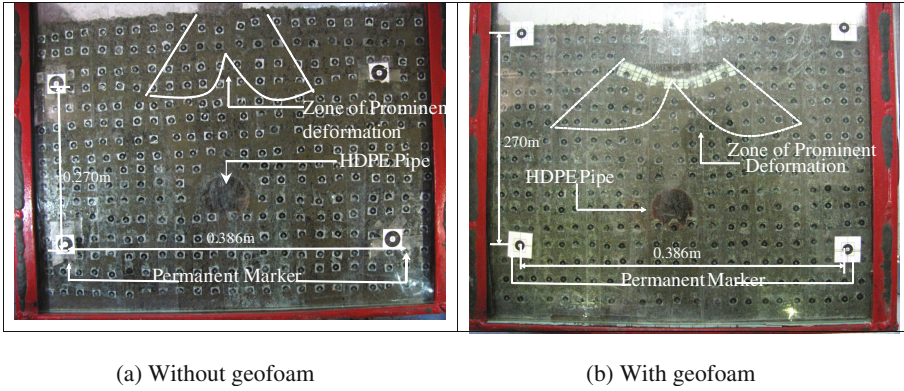


Fig. 7. Deformed profile of buried pipe and surrounding soil

7 Image Analysis

The open source software ImageJ worked on the images analysis which obtained from the test performed. The advanced template matching plugins and PIV (Particle Image Velocimetry is a velocity-measuring technique. The technique was originally implemented using double-flash photography of a seeded flow. The resulting photographs contain image pairs of each seed particle. For PIV analysis, the photograph is divided into a grid of test patches. The displacement vector of each patch during the interval between the flashes is found by locating the peak of the autocorrelation function of each patch. The peak in the autocorrelation function indicates that the two images of each seeding particle captured during the flashes are overlying each other. The correlation offset is equal to the displacement vector.) analysis are used to measure displacements, which was occurred in, above and around the pipe and geofoam. The deformed view of observational models with and without geofoam is shown in Fig. 7. With the help of image analysis throughout sequence order of images the markers were carried. In this experiment the reference markers were non-displaced and so were used to establish a benchmark for image calibration as well as to measure displacement of the movable plastic markers. When geofoam was included below the shallow, foundation deformations were observed to decrease importantly. When geofoam was introduced in the experiment geometry, the primary deforming zone was found to be concentrating in and around the foundation area. Further, these deformations were observed to be decreasing the seeable heaves at the surface level as well as the deformations in the buried pipe.

The displacement vector diagrams for buried pipeline experimental models without and with geofoam shown in Fig. 8. Comparison is made between two identical models with and without geofoam at a maximum footing settlement of 30 mm. For the improved visualization of the results the vectors in figure are scaled up two times than the original. Punching shear failure could clearly be observed when no geofoam inclusion was made. The fine grained soil deformation carry further to the buried pipe and the zone of plastic equilibrium moves away and forms a heave on both side of the

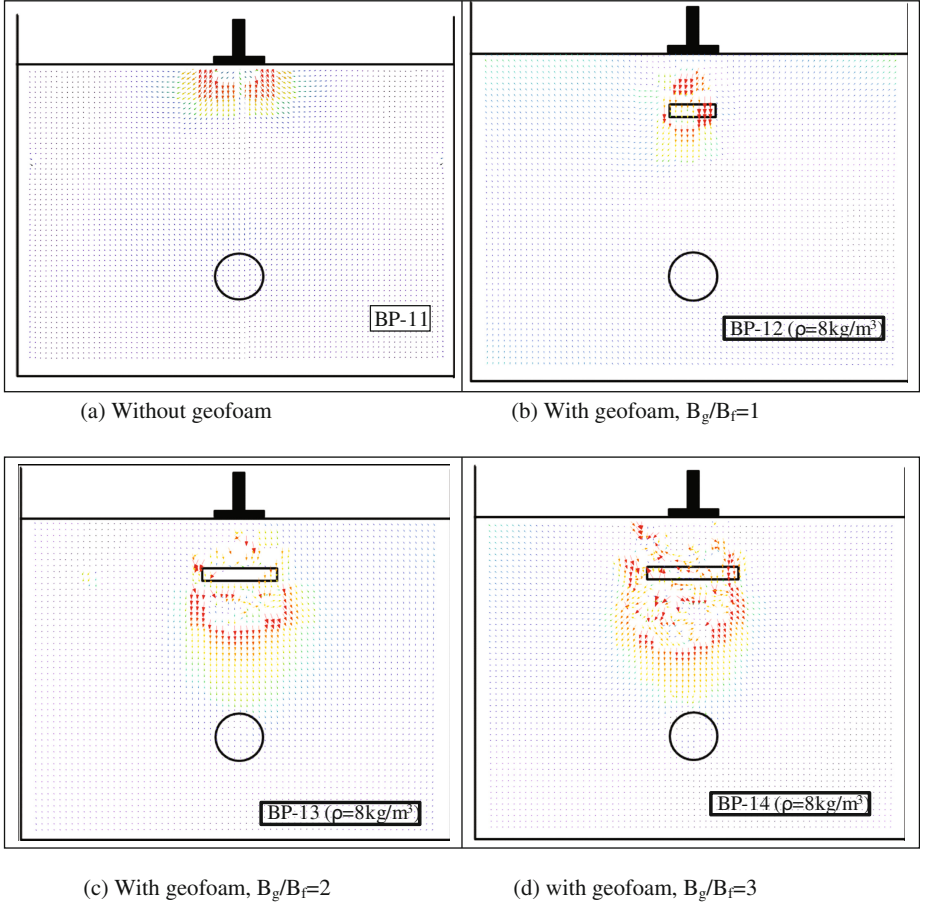
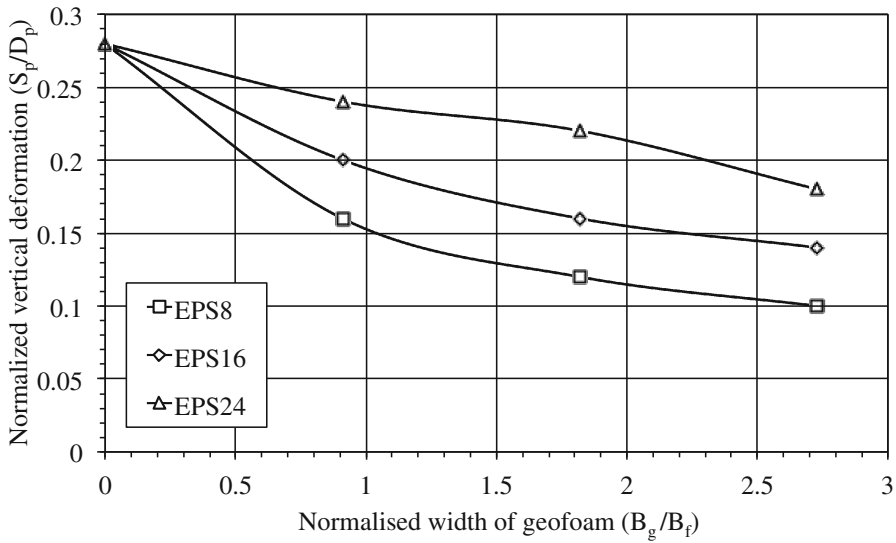
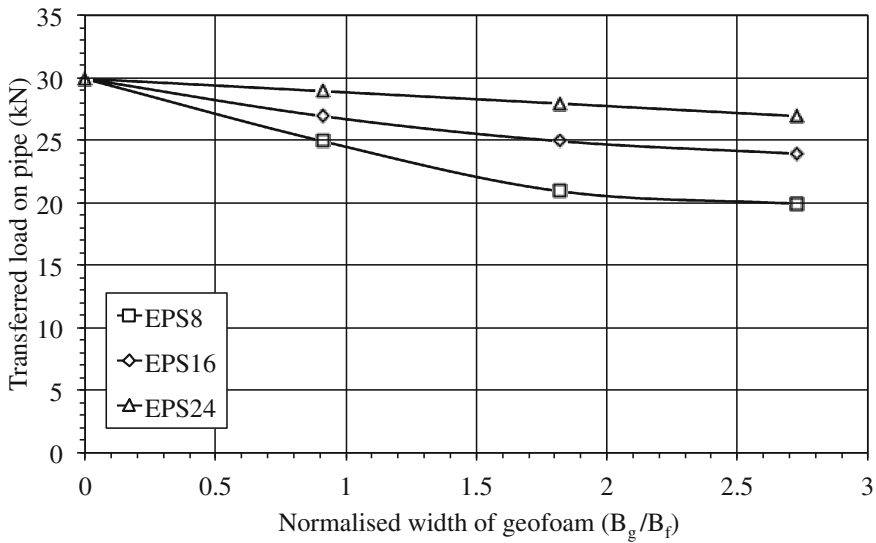


Fig. 8. Displacement vector for test models with and without geofoam

footing. It observed to decrease with increase in width of the geofoam when geofoam was placed below footing at depth B_f . When the geofoam inclusion provides a compressible bed below footing which compress allowing the load distributed forming an invert arch and load maximum at center and minimum at corner. Due to this the load transfer from axial direction to the outward diagonal directions. Majority of the movements in cohesive soil occurs well above the buried pipe at the same time. This made easier to the shear strength improvement of the cohesive soil and thus transfers reducible loads on the buried pipe.



(a) Vertical deformation in pipe



(b) Load transferred on pipe

Fig. 9. Influence of geofoam density and thickness on deformation and load transfer

8 Results and Discussion

8.1 Influence of geofoam width and geofoam density

Deformations in the vertical direction were calculated from image analysis for all the model tests performed in the present study. It was observed that the deformations in the pipe are inversely proportional to the width of the geofoam and directly proportional to the density of the geofoam. Figure 9(a) shows the variation of vertical deformation occurred in pipe with respect to the normalized width of the geofoam for varying density of the geofoam. A similar representation about the load transferred on the pipe could be made as shown in Fig. 9(b). The load transferred to the pipe was estimated based on the deformations measured through image analysis and the corresponding load from the load deformation diagram of HDPE pipe as shown in Fig. 5. The vertical axis is normalized to the pipe diameter in Fig. 9(a). A maximum reduction in load transferred of up to 32.14% was observed in case of low-density geofoam (EPS8) having maximum width of 150 mm. Table 3 summarizes the results obtained from the series of the model tests performed in this study.

Table 3. Summary of the model tests performed in the present study

Test legend	Geofoam width (mm)	Geofoam density (kg/m ³)	Vertical deformation in pipe, S_p/D_p	Load transferred on pipe (kN)
BP11	*N.A	*N.A	0.024	28
BP12	50	8	0.012	23
BP13	100		0.01	20
BP14	150		0.009	19
BP15	50	16	0.018	26
BP16	100		0.014	23
BP17	150		0.011	21
BP18	50	24	0.022	27
BP19	100		0.018	24
BP20	150		0.014	22

*Not applicable as test was performed without geofoam inclusion.

9 Conclusions

Based on the observations made in the present study, Conclusions made are as below,

1. Geofoam as a compressible inclusion placed below strip footing provides significant reduction in transferred load on buried pipes.
2. As the density of the geofoam inclusion decreases, the load on buried pipes reduces. Which means the load transferred on the buried pipes is inversely proportional to the density of the geofoam.

3. With increase in width of the geofoam load reduction increase. This is mainly due to the load dispersion over wider area in clay above the pipe. The strength of the soil mobilizes with increase in width of the geofoam. A maximum decrease of 32.14% in load on the buried pipe was obtained when a low-density (i.e. 8 kg/m^3) geofoam with maximum width of $3B_f$ was used.
4. So, A maximum reduction in load transfer on buried pipes due to surface loading can be achieved with help of low density geofoam having wider width as a compressible inclusion over the buried pipes.

9.1 Limitations

Pertaining to the fact that the small-scale modeling is associated with various limitations following limitations are described in the context of the present study.

1. Small-scale modeling does not induce the identical stress strain conditions as that of field conditions, so the results obtained and presented in this paper should be used only to understand the patterns of load distribution. To interpret the actual analysis and design values a field study or centrifuge model study is recommended.
2. Load transfer mechanism may also be the function of pipe material type and surrounding clay, so a detailed parametric study using this variable is needed to perform to arrive up to suitable implementation of geofoam in the field applications of pressure reduction.
3. The load estimate on the buried pipe was made based on isolate compression test only, however the estimates of the loads must be made based on the confined behavior of the pipe embedded in soil. So this is included in the future scope of the present study.

Acknowledgements. Author would like to thank the reviewers to invest their time and provided valuable suggestions on the improvement of the present manuscript.

References

- De Anirban, A.N.M., Zimmie, T.F.: Numerical and physical modeling of geofoam barriers as protection against effects of surface blast on underground tunnels. *Geotext. Geomembr.* **1**, 1–12 (2016)
- Bilgin, O., Stewart, H.E.: Studying buried pipeline behavior using physical and numerical modeling. In: *GeoCongress 2012: State of the Art and Practice in Geotechnical Engineering*, vol. 1, pp. 2128–2137, Oakland, California, United States (2012)
- Corey, R., Han, J., Khatri, D.K., Parsons, R.L.: Laboratory study on geosynthetic protection of buried steel reinforced HDPE pipes from static loading. *J. Geotech. Geoenvironmental Eng.* **1** (1), 1–10 (2014)
- Johnson, J., Hutson, A.C., Gibson, R.L., Verreault, L.: Protecting existing PCCP subject to external transient loads. In: *Pipelines 2010: Climbing New Peaks to Infrastructure Reliability—Renew, Rehab, and Reinvest*, vol. 1, pp. 203–210. ASCE, Keystone (2010)

- Lin, T.J., Chou, C.H.: Verification of numerical modeling in buried pipelines under large fault movements by small-scale experiments. In: Fifteenth World Conference on Earthquake Engineering, vol. 1, pp. 1–9, Lisbon, Portugal (2012)
- Stephen, S.: Contribution of lateral earth pressure resistance to restrain horizontal thrust in buried pipelines. In: Pipelines-A Sound Conduit for Sharing Solutions, vol. 1, pp. 358–371. ASCE, Carlsbad (2011)
- Watkins, R.K.: Pipe and soil mechanics for buried corrugated HDPE pipe. In: Pipelines 2004: Pipeline Engineering and Construction, vol. 1, pp. 1–10. ASCE, San Diego (2004)

Ground Improvement and Earth Structures
Proceedings of the 1st GeoMEast International
Congress and Exhibition, Egypt 2017 on Sustainable
Civil Infrastructures

Bouassida, M.; Meguid, M.A. (Eds.)

2018, VIII, 171 p. 132 illus., Softcover

ISBN: 978-3-319-63888-1